Topological phase transition and two-dimensional topological insulators in Ge-based thin films

Bahadur Singh,[1] Hsin Lin,[2,3,*] R. Prasad,[1] and A. Bansil[2]
[1]*Department of Physics, Indian Institute of Technology Kanpur, Kanpur 208016, India*
[2]*Department of Physics, Northeastern University, Boston, Massachusetts 02115, USA*
[3]*Graphene Research Centre and Department of Physics, National University of Singapore, Singapore 117542*
(Received 5 September 2013; published 25 November 2013)

We discuss possible topological phase transitions in Ge-based thin films of $Ge(Bi_xSb_{1-x})_2Te_4$ as a function of layer thickness and Bi concentration x using the first-principles density functional theory framework. The bulk material is a topological insulator at $x = 1.0$ with a single Dirac cone surface state at the surface Brillouin zone center, whereas it is a trivial insulator at $x = 0$. Through a systematic examination of the band topologies, we predict that thin films of $Ge(Bi_xSb_{1-x})_2Te_4$ with $x = 0.6$, 0.8, and 1.0 are candidates for two-dimensional (2D) topological insulators, which would undergo a 2D topological phase transition as a function of x. A topological phase diagram for $Ge(Bi_xSb_{1-x})_2Te_4$ thin films is presented to help guide their experimental exploration.

DOI: 10.1103/PhysRevB.88.195147 PACS number(s): 71.20.Nr, 71.10.Pm, 73.20.At

I. INTRODUCTION

Topological insulators (TIs) are novel materials in which even though the bulk system is insulating, the surface can support spin-polarized gapless states with Dirac-cone-like linear energy dispersion.[1–3] The topological surface states are unique in being robust against scattering from nonmagnetic impurities and display spin-momentum locking, which results in helical spin textures.[4,5] TIs not only offer exciting possibilities for applications in spintronics, energy, and information technologies, but also provide platforms for exploring in a solid-state setting questions which have traditionally been considered to lie in the realm of high-energy physics, such as the Weyl semimetal phases and the Higgs mechanism.[6–12]

Two-dimensional (2D) topological insulators, also referred to as the quantum spin Hall (QSH) insulators, were predicted theoretically before being realized experimentally in HgTe/CdTe quantum wells.[5,13] The three-dimensional (3D) TIs were identified later in bismuth-based thermoelectrics, $Bi_{1-x}Sb_x$, Bi_2Se_3, Bi_2Te_3, and Sb_2Te_3,[14–16] although transport properties of these binary TIs are dominated by intrinsic vacancies and disorder in the bulk material. By now a variety of 3D TIs have been proposed theoretically and verified experimentally in a number of cases.[17–22] In sharp contrast, to date, the only experimental realizations of the QSH state are HgTe/CdTe and InAs/GaSb/AlSb quantum well systems.[23,24] No stand-alone thin film or a thin film supported on a suitable substrate has been realized as a QSH state, although various theoretical proposals have been made suggesting that 2D TIs could be achieved through the reduced dimensionality in thin films of 3D TIs.[17,25–28] The need for finding new QSH insulator materials is for these reasons obvious.

A topological phase transition (TPT) from a trivial to a nontrivial topological phase in 2D is an interesting unexplored issue, although in 3D a TPT has been demonstrated in $TlBi(Se,S)_2$ solid solutions.[12] Despite the theoretical prediction for the existence of nontrivial 2D TIs in this family of materials,[17] no experimental realization has been reported, which may be due to stronger bonding in the Tl compounds compared to the weaker van der Waals–type bonding between quintuple layers in the Bi_2Se_3 family. Interestingly, rhombohedral Sb_2Se_3 has been predicted to be a trivial insulator, implying that a TPT could be realized in $(Bi_{1-x}Sb_x)_2Se_3$ solid solutions. However, the real Sb_2Se_3 material exhibits an orthorhombic structure, and a structural phase transition intervenes before the TPT point is reached, as the Sb concentration increases.

These considerations suggest that a strategy for realizing a thin-film material exhibiting a 2D TPT is to begin with an existing 3D topological material in which the layers are weakly bonded and trivial and nontrivial topological phases can be achieved without encountering a structural instability. Here we recall that $GeBi_2Te_4$ (GBT124) was theoretically predicted[29,30] and experimentally verified[19,31] as a 3D TI, but $GeSb_2Te_4$ (GST124) is predicted[30] to be a trivial insulator with a large bulk band gap. GBT124 and GST124 thus support different topological characters, but possess a similar lattice structure. Notably, insulating samples of Bi_2Te_3 and Bi_2Se_3 have proven difficult to realize experimentally, but this problem may prove more tractable in the $Ge(Bi_xSb_{1-x})_2Te_4$ system. In particular, the Dirac point in GBT124, for example, is well isolated from the bulk bands,[19,31] while it lies very close to the valence band maximum or it is buried in the bulk bands in Bi_2Te_3/Bi_2Se_3. Along this line, experimental studies of GBT124 show a larger surface-state spin polarization (∼70%)[30,31] compared to Bi_2Te_3 and Bi_2Se_3 (∼50%–60%).[32] Also, being ternary compounds, there is greater flexibility in substitutions, for example, the Ge site in GBT124 can be replaced by Sn or Pb to tune the lattice constant and electronic structure. GBT124 and GST124 thus are good candidate parent compounds for investigating a TPT. Also, if we consider related 2D slabs thinner than the surface-state decay length,[33,34] these slabs may yield a material supporting a 2D TI as well as a 2D TPT.[25–27] Moreover, since GBT124 is known to be n-type and topologically nontrivial, adding Sb could reduce electron carriers, leading to a more insulating compound. Accordingly, this paper examines the evolution of topological characteristics of $Ge(Bi_xSb_{1-x})_2Te_4$ by systematically varying the concentration x of Bi atoms for various layer thicknesses. We find N-layer (NL) films of $Ge(Bi_xSb_{1-x})_2Te_4$ to be 2D TIs as follows: 28L and 35L films at $x = 0.6$; 21L, 28L, and 35L films at $x = 0.8$; and 14L, 21L, and 28L films at $x = 1.0$. The material undergoes a 3D phase transition to topological regime

near $x = 0.6$. We have also constructed a topological phase diagram for 2D $Ge(Bi_xSb_{1-x})_2Te_4$ thin films with varying thickness and Bi concentrations.

The present article is organized as follows. Section II gives computational details. In Sec. III, we delineate the bulk crystal and electronic structures of GBT124 and GST124. The TPT in $Ge(Bi_xSb_{1-x})_2Te_4$ with varying x and the existence of 2D TIs in thin films of $Ge(Bi_xSb_{1-x})_2Te_4$ with various concentrations are also discussed. Finally, Sec. IV summarizes our conclusions.

II. COMPUTATIONAL DETAILS

Our electronic structure calculations were carried out within the density functional theory (DFT)[35] framework with the projector-augmented-wave (PAW) basis.[36,37] The generalized-gradient approximation (GGA)[38] was used to include exchange-correlation effects, and the spin-orbit coupling (SOC) effects were included as implemented in VASP (Vienna Ab Initio Simulation Package).[36] The bulk calculations used a plane-wave cut-off energy of 350 eV and a Γ-centered $8 \times 8 \times 8$ k mesh with a conjugate gradient algorithm.[39] Since Sb and Bi atoms possess a similar outermost electronic configuration, evolution of electronic structure could be tracked by varying either Bi or Sb concentration, and we have chosen to do so by varying the concentration of Bi atoms for the sake of definiteness. Specifically, a bulk hexagonal supercell with 35 atomic layers (five septuple layers) was prepared with values of x varying between 0.0 and 1.0. The corresponding bulk parameters, including the structure, were optimized until all components of Hellman-Feynman forces on each ion were less than 0.001 eV/Å. The relaxed structures of $Ge(Bi_xSb_{1-x})_2Te_4$ examined for various Bi concentrations were also found to be hexagonal. The surface electronic-structure calculations are based on a slab geometry with a plane-wave cut-off energy of 350 eV, a Γ-centered $8 \times 8 \times 1$ k mesh, and relaxed bulk parameters with a vacuum greater than 12 Å.

III. RESULTS AND DISCUSSIONS

A. Bulk crystal and band structure

The GBT124 and GST124 belong to the rhombohedral crystal structure,[19,30,31] composed of seven-layer (7L) or septuple blocks, with layers in the sequence Te-Bi(Sb)-Te-Ge-Te-Bi(Sb)-Te. As an example, the arrangement of layers in a unit cell in GBT124 is shown in Fig. 1(a). In a septuple block, the Ge and Bi atoms are sandwiched between the Te atoms, and the Ge atom can be chosen as the inversion center. The bonding within the septuple blocks is strong, being mainly of ionic-covalent type, whereas across the septuple blocks bonding is of van der Waals type.[19,31] With this in mind, we take the surface termination to occur between two septuple blocks and regard one septuple block as a 2D thin film with the smallest thickness considered.

The bulk band structures of GBT124 and GST124 are shown in Figs. 1(c) and 1(d), respectively. GBT124 is an indirect band-gap semiconductor in which the conduction band minimum (CBM) and valence band maxima (VBM) lie along the $\Gamma - Z$ direction. The bulk valence and conduction bands

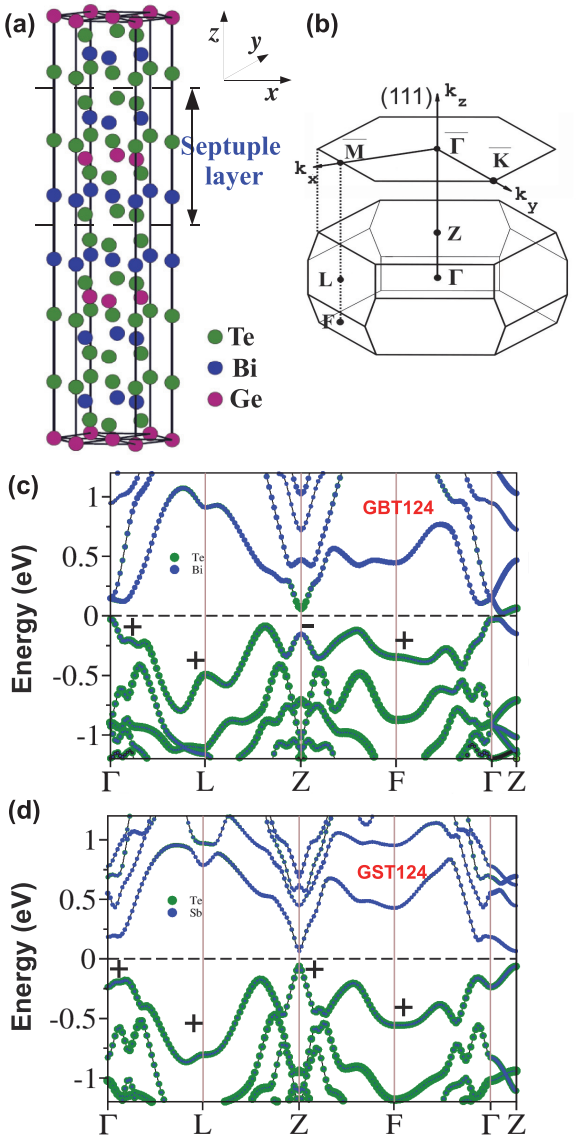

FIG. 1. (Color online) (a) Bulk crystal structure of $GeBi_2Te_4$ (GBT124) with inversion symmetry. A seven-atomic-layer block is shown. (b) The corresponding bulk Brillouin zone (BZ) with four time-reversal invariant points Γ, F, Z, and L, and the 2D Brillouin zone of the (111) surface with two time-reversal invariant points $\overline{\Gamma}$ and $\overline{M}$. (c, d) The bulk electronic structure of $GeBi_2Te_4$(GBT124) and $GeSb_2Te_4$(GST124), respectively, with Bi/Sb (blue dots) and Te (green dots) atomic weights for different bands. Signs of $\delta_i = \pm 1$ at TRIM are also shown.

at the Z point are composed of Bi p states and Te p states, respectively, with an inverted band order. In contrast, GST124 is a direct band-gap material with CBM and VBM at Z point and a normal ordering of bands. Since the structure possesses inversion symmetry in both cases, it is possible to calculate the Z_2 invariants $\nu_0;(\nu_1\nu_2\nu_3)$ (where ν_0 is a strong and $\nu_{k=1,2,3}$ is a weak topological invariant)[40] from the bulk band structure. The Z_2 invariants are determined from the parity $\xi_m(\Gamma_i)$ of the occupied bulk bands at the time-reversal invariant momentum (TRIM) points $\Gamma_{i=(n_1n_2n_3)} = (n_1b_1 + n_2b_2 + n_3b_3)/2$, where b_1, b_2, and b_3 are the reciprocal lattice vectors and

$n_k = 0$ or 1.[40] The Z_2 invariants can then be calculated using

$$(-1)^{\nu_0} = \prod_{i=1}^{8} \delta_i \tag{1}$$

and

$$(-1)^{\nu_k} = \prod_{n_k=1; n_{j\neq k}=0,1} \delta_{i=(n_1,n_2,n_3),} \tag{2}$$

where

$$\delta_i = \prod_{m=1}^{N} \xi_{2m}(\Gamma_i). \tag{3}$$

Here, N is the number of occupied bulk bands and $\xi_{2m}(\Gamma_i) = \pm 1$ is the parity of the $2m$th occupied energy band at the point Γ_i. There are eight TRIM points in the rhombohedral Brillouin zone but only four of these points [Γ, Z, F, and L; see Fig. 1(b)] are inequivalent. The product of the parity eigenvalues ($\delta_i = \pm 1$) of the occupied bands at the TRIM points are shown in Figs. 1(c)–1(d). In the case of GBT124, interestingly, the band inversion occur at the Z point, which leads to Z_2 invariants being equal to 1;(111), and is different from Bi_2Se_3 TI family,[14] where the band inversion occurs at the Γ point, yielding Z_2 invariants to be 1;(000). On other hand, GST124 lacks band inversion at any of the TRIM points, indicating that the system is a normal insulator with all Z_2 invariants zero.

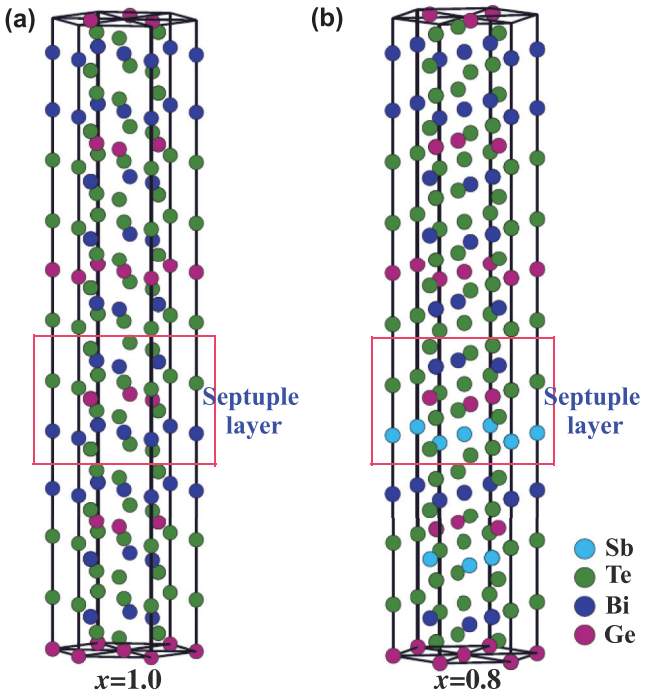

FIG. 2. (Color online) Schematic diagram of the bulk hexagonal supercell with 35 atomic layers for (a) $x = 1.0$ (with inversion symmetry) and (b) $x = 0.8$ (without inversion symmetry). Red boxes identify the septuple layer arrangement.

B. Surface band structures and 3D topological phase transition

For investigating the TPT in $Ge(Bi_xSb_{1-x})_2Te_4$ compounds, we used a supercell geometry with a relaxed hexagonal supercell having 35 atomic layers for $x = 0.0, 0.2, 0.4, 0.5, 0.6, 0.8$, and 1.0.[41–43] As examples, the bulk hexagonal supercells for $x = 1.0$ and $x = 0.8$ are shown in Fig. 2. For $x = 1.0$, the Ge atom in the supercell remains an inversion center, whereas for $x = 0.8$ this is not the case and the inversion symmetry is broken.

The bulk band structures were computed using the fully relaxed structures. Figure 3(a) shows the variation of bulk band gap of $Ge(Bi_xSb_{1-x})_2Te_4$ as a function of x. The gap is seen to start decreasing from 0.13 eV at $x = 0.0$, with the valence band and conduction band mainly composed of Te p states and Bi/Sb p states, respectively [Fig. 3(b)], to a minimum value around $0.5 < x < 0.6$. As we further increase x, the gap opens up again and attains a value of $\approx$0.07 eV at $x = 1.0$, with valence and conduction bands swapping their orbital characters at the Z point. This closing and reopening of the bulk gap with an inverted band order indicates that there is a TPT between $x = 0.5$–0.6.[44,45]

Figures 3(c)–3(h) show electronic structures of 35-atomic-layer slabs for various Bi concentrations. Figure 3(c) shows that the $x = 0.0$ compound GST124 is a normal insulator with a large band gap without a gapless surface state inside the bulk energy gap region, which is consistent with the trivial insulator found in bulk calculations. On the other hand, a clear Dirac cone surface state at the $\bar{\Gamma}$ point is seen in Fig. 3(h) for the nontrivial phase GBT124 at $x = 1$. The system becomes metallic at $x = 0.2$ and 0.4 due to a surface conduction band crossing the Fermi level. Between the $\bar{\Gamma}$ point and the $\bar{M}$ point, this surface band crosses the Fermi level twice, an even number, consistent with the trivial phase found in bulk calculations. The metallic character decreases with increasing x and at $x = 0.6$ and 0.8, it becomes insulating with a very small gap ($\approx$10 and 18 meV at $x = 0.6$ and 0.8, respectively). This gap is due to quantum confinement effects, i.e., the interaction between the two Dirac cones residing on the top and bottom surfaces. Without such interaction, each side of the surface has gapless Dirac cone surface states centered at the $\bar{\Gamma}$ point, which arises from the nontrivial bulk band topology.

C. 2D topological insulators

We now turn to discuss the evolution of electronic structure with slab thickness in terms of multiples of septuple layer blocks. Reference 34 has previously shown that when the thickness of a slab is smaller than the surface-state decay length, states on the two surfaces of the slab become coupled via quantum tunneling, leading to a small thickness-dependent gap in the electronic structure.[10,27,46] This coupling between the two surfaces for thin slabs is responsible for opening a gap at the Dirac point and is the key for realizing the insulating phase. Since thin films of $Ge(Bi_xSb_{1-x})_2Te_4$ with $x = 0.0$ (GST124) as well as $x = 1.0$ (GBT124) [Fig. 2(a)] are symmetric under inversion, we used parity analysis[40] to determine their topological character. On the other hand, thin films for $x = 0.2$, 0.4, 0.5, 0.6, and 0.8 are asymmetric under inversion [Fig. 2(b)], and therefore parity analysis cannot be

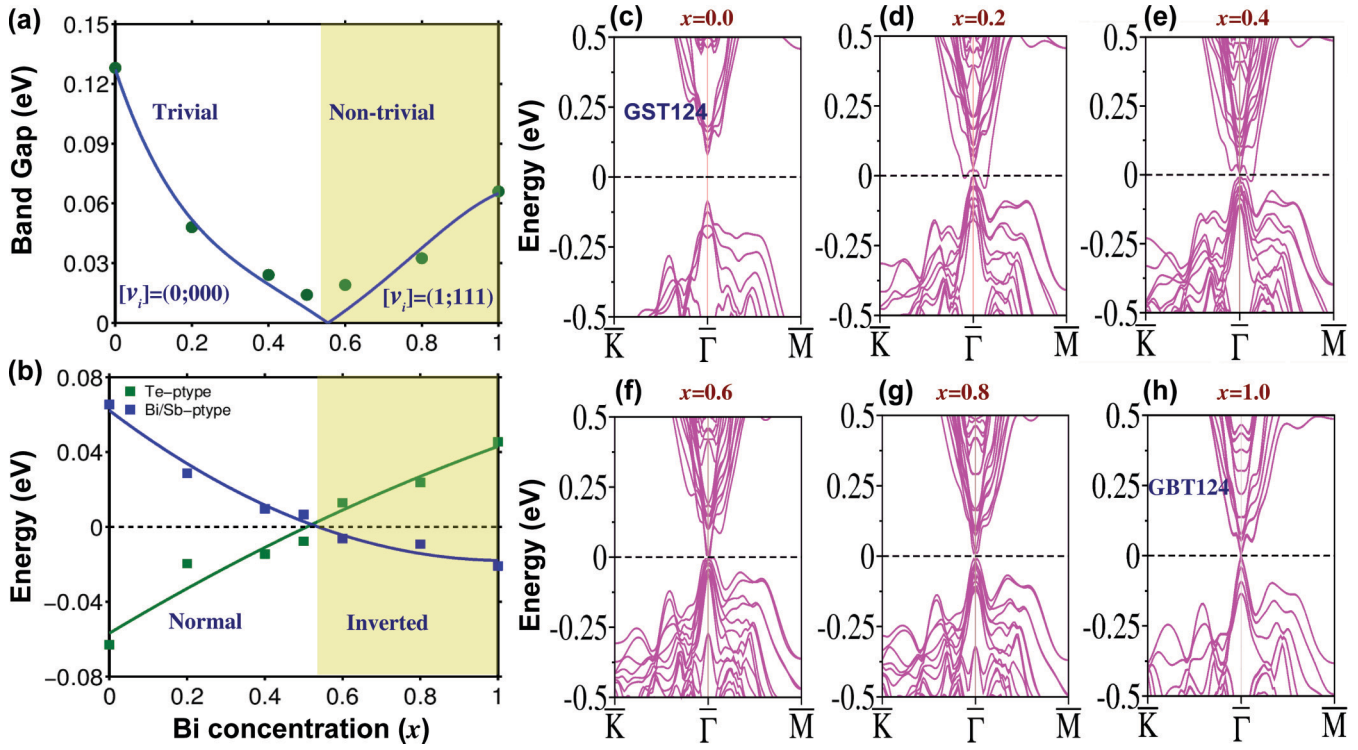

FIG. 3. (Color online) (a) Variation of band gap of bulk hexagonal supercell of $Ge(Bi_xSb_{1-x})_2Te_4$ with x. The related topological invariants are shown. Blue line is a guide to the eye. (b) Evolution of Te p-type (green points) and Bi/Sb p-type (blue points) valence band maximum and conduction band minimum at the Z point with x. The valence and conduction bands are seen to be inverted between $0.5 < x < 0.6$. Green and blue lines are guides to the eye. Panels (c)−(h) show the surface electronic structures for various x values. There is a phase transition from normal insulator (NI) to topological insulator (TI) near $x = 0.6$, although a small gap is seen at $x = 0.6$ and 0.8, making these compositions suitable candidates for realizing 2D TIs. The dashed zero lines mark the Fermi energy.

used. Instead, we varied the SOC strength and monitor the band gap to assess the topological character. We have further verified this nontrivial character via edge-state computations.

Figures 4(a)–4(d) show electronic structures of GBT124 films ($x = 1.0$) for various thicknesses. It is evident that the slab with 7L displays an indirect band gap, whereas thicker slabs with 14L, 21L, and 28L have a direct band gap. Since all these slabs are insulating, we examined the possibility of these slabs being 2D TIs. Note that slabs with $x = 1.0$ are symmetric under inversion, so that the Bloch wave functions have well-defined parity at the TRIM points, which can be used to compute the 2D topological invariants, shown in Figs. 4(a)–4(d). The 2D Z_2 invariant assumes the nontrivial value equal to 1 for 14L, 21L, and 28L films but has the trivial value of zero for the 7L film.

As already pointed out, thin films with $x = 0.2, 0.4, 0.5, 0.6$, and 0.8 are asymmetric under inversion. In order to check their topological character, we varied the SOC strength from zero to 100%. Since the topological phase for all insulators without SOC is trivial, we can monitor the gap size to determine if a TPT takes place as the strength of the SOC is increased. Results for $x = 0.8$ are shown in Fig. 4(e). For 7L and 14L films, the band gap decreases with increasing values of the SOC strength, being 0.336 eV for 7L and 0.019 eV for 14L at 100% SOC without closing at any value of SOC strength. Therefore, band structures with and without SOC are adiabatically connected, implying that they are both topologically trivial. On the other hand, for 21L, 28L, and 35L films, the gap closes at 86%, 84%, and 89% SOC strength, respectively, and reopens to a value of 0.071 eV for 21L, 0.062 eV for 28L, and 0.032 eV for the 35L film at 100% SOC strength. We thus conclude that the slabs of $Ge(Bi_xSb_{1-x})_2Te_4$ at $x = 0.8$, with 21L, 28L, and 35L thickness, are topologically nontrivial.

The existence of gapless edge states is the hallmark of 2D topological insulators. Thus to verify the topological character of 2D thin films of $Ge(Bi_xSb_{1-x})_2Te_4$, we also computed the edge-state energy dispersion for inversion-symmetric ($x = 1.0$) and inversion-asymmetric ($x = 0.8$) slabs. As an example, the unit cell for edge-state computations of GBT124 ($x = 1.0$) is shown in Fig. 5(a), where the two edges considered are marked with pink and green vertical lines. The edge-state energy dispersion in GBT124 ($x = 1.0$) for 14L [Fig. 5(b)] shows that there are three Fermi level crossings, labeled by {1,2,3}. This odd number of crossings between two time-reversal invariant points confirms the nontrivial nature of these films. We also computed the edge states of $Ge(Bi_xSb_{1-x})_2Te_4$ with $x = 0.8$ for 21L and the results are shown in Fig. 5(c). Since these slabs are asymmetric under inversion, the states associated with opposite edges are not degenerate. The labels {1,2,3} and {1′,2′,3′} in Fig. 5(c) indicate the Fermi-level crossings from states related to the left and right edges, respectively. In this case also the edge states cross the Fermi level three times, implying that these thin films are topologically nontrivial.

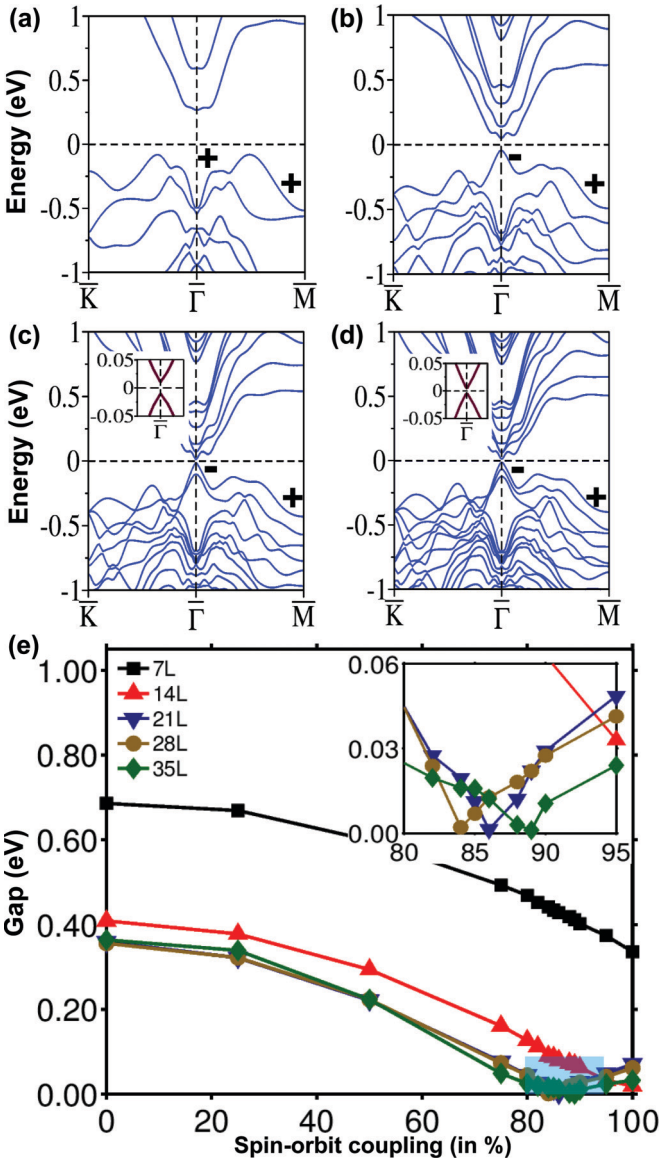

FIG. 4. (Color online) Electronic structure of $Ge(Bi_xSb_{1-x})_2Te_4$ at $x = 1.0$ for (a) 7L, (b) 14L, (c) 21L, and (d) 28L thick films. Signs of $\delta_i = \pm 1$ at the TRIM points of the 2D Brillouin zone are also shown. Panel (e) shows the variation of band gap for various film thicknesses in $Ge(Bi_xSb_{1-x})_2Te_4$ at $x = 0.8$ as a function of the size of spin-orbit coupling. The inset zooms in on the shaded region. The energy gap decreases to zero and reopens as SOC increases from zero to 100% for 21L, 28L, and 35L slabs.

In order to explore topological phases of 2D $Ge(Bi_xSb_{1-x})_2Te_4$ films, we carried out calculations for 7L, 14L, 21L, 28L, and 35L slabs for $x = 0.0, 0.2, 0.4, 0.5, 0.6, 0.8$, and 1.0. The topological nature of the films was determined by the methods already described above. The computed variation of the band gap at the $\overline{\Gamma}$ point for slabs of different thicknesses and compositions is summarized in Fig. 5(d). The shaded area in the figure identifies slabs with nontrivial character. All slabs at $x = 0.0$ (GST124) are topologically trivial. Excepting the 7L film, thin films for $x = 0.2$, 0.4, and 0.5 are metallic, where the metallic character decreases with increasing Bi concentration. An insulating phase is found

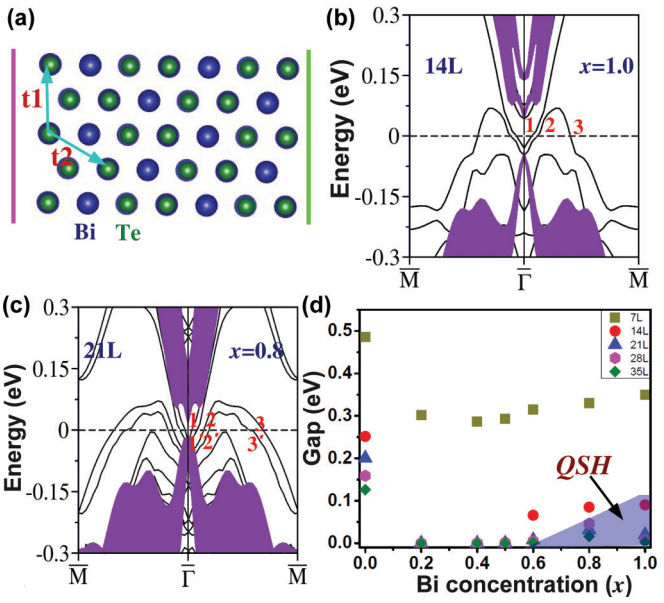

FIG. 5. (Color online) (a) Top view of 2D thin films of GBT124 with in-plane lattice vectors **t1** and **t2**. The edge states have been computed along the edges shown by pink and green lines. The edge states for (b) 14L GBT124 and (c) for 21L $Ge(Bi_xSb_{1-x})_2Te_4$ at $x = 0.8$. The continuum of surface bands is shown in violet color. An odd number of crossings of the edge states at the Fermi level establishes their nontrivial character. (d) Band gaps of slabs with various thicknesses and Bi concentrations x. Shaded region shows slabs which are nontrivial and predicted to provide new candidates for realizing 2D TIs.

for slabs with larger values of x. In particular, we predict that the 28L and 35L films for $x = 0.6$, 21L, 28L, and 35L films for $x = 0.8$, and 14L, 21L, and 28L films with $x = 1.0$ are topologically nontrivial. Thus these slabs are possible candidates for realizing 2D TIs, and their solid solutions could realize a 2D TPT.

IV. SUMMARY AND CONCLUSIONS

We have investigated electronic structures of thin films of a Ge-based system $Ge(Bi_xSb_{1-x})_2Te_4$ over the full range of Bi concentrations x within the framework of the density functional theory. By using parity analysis and surface-state computations, we show that the $x = 1.0$ bulk compound, GBT124, is a topological insulator with $Z_2 = 1;(111)$ harboring a single metallic Dirac cone surface state at the $\overline{\Gamma}$ point lying within the bulk energy gap. On the other extreme, at $x = 0$, the material (GST124) transforms into a trivial insulator without metallic surface states. Computations as a function of x indicate that a topological phase transition (TPT) takes place for x values between 0.5 and 0.6. Our analysis further suggests that a 2D-TPT could be realized in thin films of $Ge(Bi_xSb_{1-x})_2Te_4$ by varying Bi concentration. We predict that 28L and 35L films at $x = 0.6$; 21L, 28L, and 35L films at $x = 0.8$; and 14L, 21L, and 28L films at $x = 1.0$ would be 2D TIs. Our study opens up the possibility of identifying the QSH state in thin films of a large materials family, along with that of realizing a 2D topological phase transition.

ACKNOWLEDGMENTS

This work was supported by the Department of Science and Technology, New Delhi (India) through project SR/S2/CMP-0098/2010. The work at Northeastern University was supported by the US Department of Energy, Office of Science, Basic Energy Sciences Contract No. DE-FG02-07ER46352, and benefited from Northeastern University's Advanced Scientific Computation Center (ASCC), theory support at the Advanced Light Source, Berkeley, and the allocation of time at the NERSC supercomputing center through DOE Grant No. DE-AC02-05CH11231. H.L. acknowledges the Singapore National Research Foundation (NRF) for support under NRF Award No. NRF-NRFF2013-03.

*nilnish@gmail.com

[1]X.-L. Qi and S.-C. Zhang, Rev. Mod. Phys. **83**, 1057 (2011).
[2]M. Z. Hasan and C. L. Kane, Rev. Mod. Phys. **82**, 3045 (2010).
[3]J. E. Moore, Nature (London) **464**, 194 (2010).
[4]B. A. Bernevig and S.-C. Zhang, Phys. Rev. Lett. **96**, 106802 (2006).
[5]B. A. Bernevig, T. L. Hughes, and S.-C. Zhang, Science **314**, 1757 (2006).
[6]X. Wan, A. M. Turner, A. Vishwanath, and S. Y. Savrasov, Phys. Rev. B **83**, 205101 (2011).
[7]A. A. Burkov and L. Balents, Phys. Rev. Lett. **107**, 127205 (2011).
[8]G. B. Halász and L. Balents, Phys. Rev. B **85**, 035103 (2012).
[9]S. Murakami, New J. Phys. **9**, 356 (2007).
[10]B. Singh, A. Sharma, H. Lin, M. Z. Hasan, R. Prasad, and A. Bansil, Phys. Rev. B **86**, 115208 (2012).
[11]T. Sato, K. Segawa, K. Kosaka, S. Souma, K. Nakayama, K. Eto, T. Minami, Y. Ando, and T. Takahashi, Nat. Phys. **7**, 840 (2011).
[12]S.-Y. Xu, Y. Xia, L. A. Wray, S. Jia, F. Meier, J. H. Dil, J. Osterwalder, B. Slomski, A. Bansil, H. Lin, R. J. Cava, and M. Z. Hasan, Science **332**, 560 (2011).
[13]M. König, S. Wiedmann, C. Brüne, A. Roth, H. Buhmann, L. W. Molenkamp, X.-L. Qi, and S.-C. Zhang, Science **318**, 766 (2007).
[14]H. Zhang, C.-X. Liu, X.-L. Qi, X. Dai, Z. Fang, and S.-C. Zhang, Nat. Phys. **5**, 438 (2009).
[15]D. Hsieh, D. Qian, L. Wray, Y. Xia, Y. S. Hor, R. J. Cava, and M. Z. Hasan, Nature (London) **452**, 970 (2008).
[16]Y. Xia, D. Qian, D. Hsieh, L. Wray, A. Pal, H. Lin, A. Bansil, D. Grauer, Y. S. Hor, R. J. Cava, and M. Z. Hasan, Nat. Phys. **5**, 398 (2009).
[17]H. Lin, R. S. Markiewicz, L. A. Wray, L. Fu, M. Z. Hasan, and A. Bansil, Phys. Rev. Lett. **105**, 036404 (2010).
[18]H. Lin, T. Das, L. A. Wray, S.-Y. Xu, M. Z. Hasan, and A. Bansil, New J. Phys. **13**, 095005 (2011).
[19]M. Neupane, S.-Y. Xu, L. A. Wray, A. Petersen, R. Shankar, N. Alidoust, C. Liu, A. Fedorov, H. Ji, J. M. Allred, Y. S. Hor, T.-R. Chang, H.-T. Jeng, H. Lin, A. Bansil, R. J. Cava, and M. Z. Hasan, Phys. Rev. B **85**, 235406 (2012).
[20]S. V. Eremeev, G. Landolt, T. V. Menshchikova, B. Slomski, Y. M. Koroteev, Z. S. Aliev, M. B. Babanly, J. Henk, A. Ernst, L. Patthey, A. Eich, A. A. Khajetoorians, J. Hagemeister, O. Pietzsch, J. Wiebe, R. Wiesendanger, P. M. Echenique, S. S. Tsirkin, I. R. Amiraslanov, J. H. Dil, and E. V. Chulkov, Nat. Commun. **3**, 635 (2012).
[21]H. Lin, L. A. Wray, Y. Xia, S. Xu, S. Jia, R. J. Cava, A. Bansil, and M. Z. Hasan, Nat. Mater. **9**, 546 (2010).
[22]K. Yang, W. Setyawan, S. Wang, M. Buongiorno Nardelli, and S. Curtarolo, Nat. Mater. **11**, 614 (2012).
[23]C. Liu, T. L. Hughes, X.-L. Qi, K. Wang, and S.-C. Zhang, Phys. Rev. Lett. **100**, 236601 (2008).
[24]I. Knez, R.-R. Du, and G. Sullivan, Phys. Rev. Lett. **107**, 136603 (2011).
[25]I. Silkin, Y. Koroteev, S. Eremeev, G. Bihlmayer, and E. Chulkov, JETP Lett. **94**, 217 (2011).
[26]C.-X. Liu, H. J. Zhang, B. Yan, X.-L. Qi, T. Frauenheim, X. Dai, Z. Fang, and S.-C. Zhang, Phys. Rev. B **81**, 041307 (2010).
[27]Y. Zhang, K. He, C.-Z. Chang, C.-L. Song, L.-L. Wang, X. Chen, J.-F. Jia, Z. Fang, X. Dai, W.-Y. Shan, S.-Q. Shen, Q. Niu, X.-L. Qi, S.-C. Zhang, X.-C. Ma, and Q.-K. Xue, Nat. Phys. **6**, 584 (2010).
[28]F.-C. Chuang, C.-H. Hsu, C.-Y. Chen, Z.-Q. Huang, V. Ozolins, H. Lin, and A. Bansil, Appl. Phys. Lett. **102**, 022424 (2013).
[29]T. Menshchikova, S. Eremeev, Y. Koroteev, V. Kuznetsov, and E. Chulkov, JETP Lett. **93**, 15 (2011).
[30]S.-Y. Xu, L. A. Wray, Y. Xia, R. Shankar, A. Petersen, A. Fedorov, H. Lin, A. Bansil, Y. S. Hor, D. Grauer, R. J. Cava, and M. Z. Hasan, arXiv:1007.5111v1.
[31]K. Okamoto, K. Kuroda, H. Miyahara, K. Miyamoto, T. Okuda, Z. S. Aliev, M. B. Babanly, I. R. Amiraslanov, K. Shimada, H. Namatame, M. Taniguchi, D. A. Samorokov, T. V. Menshchikova, E. V. Chulkov, and A. Kimura, Phys. Rev. B **86**, 195304 (2012).
[32]Oleg V. Yazyev, Joel E. Moore, and Steven G. Louie, Phys. Rev. Lett. **105**, 266806 (2010).
[33]B. Zhou, H.-Z. Lu, R.-L. Chu, S.-Q. Shen, and Q. Niu, Phys. Rev. Lett. **101**, 246807 (2008).
[34]M. Wada, S. Murakami, F. Freimuth, and G. Bihlmayer, Phys. Rev. B **83**, 121310 (2011).
[35]P. Hohenberg and W. Kohn, Phys. Rev. **136**, B864 (1964).
[36]G. Kresse and J. Furthmüller, Phys. Rev. B **54**, 11169 (1996).
[37]G. Kresse and D. Joubert, Phys. Rev. B **59**, 1758 (1999).
[38]J. P. Perdew, K. Burke, and M. Ernzerhof, Phys. Rev. Lett. **77**, 3865 (1996).
[39]W. H. Press, B. P. Flannery, S. A. Teukolsky, and W. T. Vetterling, *Numerical Recipes* (Cambridge University Press, New York, 1986).
[40]L. Fu and C. L. Kane, Phys. Rev. B **76**, 045302 (2007).
[41]Note that we have modeled nonstoichiometric compositions by using appropriate supercells of ordered phases. It will be interesting to consider disorder effects using first-principles approaches within the DFT framework (Ref. 42), although the virtual crystal approximation (Ref. 43) might provide a reasonable scheme for describing effects of Bi/Sb substitution.
[42]A. Bansil, Phys. Rev. B **20**, 4025 (1979); **20**, 4035 (1979); L. Schwartz and A. Bansil, *ibid.* **10**, 3261 (1974).

[43] A. Bansil, Z. Naturforsch. A **48**, 165 (1993); H. Lin, S. Sahrakorpi, R. S. Markiewicz, and A. Bansil, Phys. Rev. Lett. **96**, 097001 (2006).

[44] Since DFT correctly predicts that $Ge(Bi_xSb_{1-x})_2Te_4$ is a trivial insulator at $x = 0$ and a nontrivial insulator at $x = 1$, we can have confidence in the prediction that a transition will take place for some value of x over the range 0–1, uncertainty in estimating the precise transition point due to inherent limitations of the DFT in underestimating gap sizes notwithstanding.

[45] Figure 3(b) indicates that the error in estimating the transition point will depend on details of how the corrections to the DFT affect the valence and conduction levels. For example, if the positions of the conduction and valence levels should undergo similar corrections (compared to the DFT) as a function of x, we may see relatively little change in the transition point in Fig. 3(b).

[46] K. Park, J. J. Heremans, V. W. Scarola, and D. Minic, Phys. Rev. Lett. **105**, 186801 (2010).